

# Quench dynamics of Rényi negativities and the quasiparticle picture

Sara Murciano<sup>1</sup>, Vincenzo Alba<sup>2,3</sup>, and Pasquale Calabrese<sup>1,4</sup>

<sup>1</sup>SISSA and INFN Sezione di Trieste, via Bonomea 265, 34136 Trieste, Italy

<sup>2</sup>Institute for Theoretical Physics, Universiteit van Amsterdam, Science Park 904, Postbus 94485, 1098 XH Amsterdam, The Netherlands

<sup>3</sup>Dipartimento di Ingegneria Industriale, Università degli Studi di Salerno, Via Giovanni Paolo II, 132 I-84084 Fisciano (SA), Italy

<sup>3</sup> International Centre for Theoretical Physics (ICTP), Strada Costiera 11, 34151 Trieste, Italy

## Abstract

The study of the moments of the partially transposed density matrix provides a new and effective way of detecting bipartite entanglement in a many-body mixed state. This is valuable for cold-atom and ion-trap experiments, as well as in the general context of quantum simulation of many-body systems. In this work we study the time evolution after a quantum quench of the moments of the partial transpose, and several related quantities, such as the Rényi negativities. By combining Conformal Field Theory (CFT) results with integrability, we show that, in the space-time scaling limit of long times and large subsystems, a quasiparticle description allows for a complete understanding of the Rényi negativities. We test our analytical predictions against exact numerical results for free-fermion and free-boson lattice models, even though our framework applies to generic interacting integrable systems.

# Contents

<b>1</b>	<b>Introduction</b>	<b>2</b>
<b>2</b>	<b>Entanglement measures for mixed states</b>	<b>4</b>
2.1	Entanglement in mixed states and logarithmic negativity . . . . .	4
2.2	Entanglement detection through partial transpose moments . . . . .	6
<b>3</b>	<b>Quench dynamics of Rényi negativities in conformal field theory</b>	<b>6</b>
3.1	Rényi negativities from twist field correlation functions . . . . .	6
3.2	Out-of-equilibrium dynamics of the Rényi negativities . . . . .	7
<b>4</b>	<b>Quasiparticle picture for the Rényi negativities in integrable systems</b>	<b>9</b>
4.1	Quasiparticle picture . . . . .	9
4.2	The quasiparticle description for Rényi negativities . . . . .	10
<b>5</b>	<b>Time evolution of Rényi negativities in free models: Numerical results</b>	<b>12</b>
5.1	Mass quench in the harmonic chain . . . . .	12
5.2	Quench in a free fermion chain . . . . .	13
5.3	Quasiparticle prediction for the $p_n$ -PPT conditions . . . . .	16
<b>6</b>	<b>Conclusions</b>	<b>17</b>

## 1 Introduction

During the last decades, the study of entanglement became a powerful tool to explore the out of equilibrium dynamics of quantum systems. The simplest and most broadly studied protocol is the quantum quench [1, 2]: a system is prepared in the ground state of a translationally invariant Hamiltonian, and at a given time a sudden change modifies the Hamiltonian. In integrable systems, the entanglement dynamics after a quench is captured by a well-known quasiparticle picture [3–6]. The key tenet of the quasiparticle picture is that the entanglement dynamics is described by the ballistic propagation of pairs of entangled excitations, which are produced after the quench (see Fig. 1). An intense theoretical activity was accompanied by a remarkable experimental progress, e.g., to measure the many-body entanglement of non-equilibrium states [7–10]. For closed bipartite systems, the von Neumann and the Rényi entropies of reduced density matrices can be used as *bona fide* measures of the entanglement shared between the two complementary parts. On the other hand, neither the entropies, nor the associated mutual information can be used to quantify the entanglement between two noncomplementary subsystems (see Fig. 1 for the situation with two disjoint sets in a one-dimensional system). The reason is that the state of the two subsystems is in general a mixed one. In this situation, the entanglement can be understood via the *partial transpose* of the reduced density matrix (RDM) which is defined as follows. Given the RDM  $\rho_A$  of a subsystem  $A = A_1 \cup A_2$  (see Fig. 1), obtained after tracing out the rest of the system  $B$  as  $\rho_A \equiv \text{Tr}_B \rho$ , the partial transpose  $\rho_A^{T_1}$  is obtained by taking the matrix transposition with respect to the degrees of freedom of one of the two subsystems (say  $A_1$ ). The key point now is that the presence of negative eigenvalues in the spectrum of  $\rho_A^{T_1}$  is a sufficient condition for  $A_1$  and  $A_2$  to be entangled [11, 12]. These negative eigenvalues are witnessed by the (logarithmic) negativity  $\mathcal{E} \equiv \ln \text{Tr} |\rho_A^{T_1}|$  [13] which turns out also to be an entanglement monotone [14].

Unfortunately, computing the negativity or measuring it experimentally in quantum many-body systems is a daunting task. This fact sparked a lot of activity aiming at finding alternative entanglement witnesses for mixed states always starting from the partially transposed RDM. To this aim, several protocols to measure the moments  $\text{Tr}(\rho_A^{T_1})^n$  of the partial transpose have

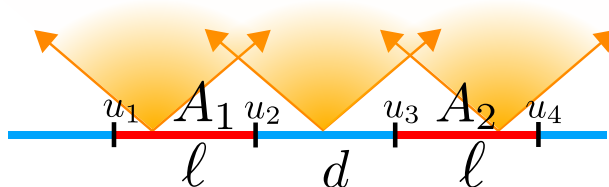


**Figure 1:** Quasiparticle picture for the time evolution after a quench of the entanglement between two disjoint intervals ( $A_1 = [u_1, u_2]$  and  $A_2 = [u_3, u_4]$ ) embedded in the infinite line. Pairs of entangled quasiparticles are emitted from every point in space at  $t = 0$ . At a given time  $t$  the entanglement between  $A$  and the remainder is proportional to the number of pairs shared between  $A$  and its complement. Similarly, the entanglement between  $A_1$  and  $A_2$  is proportional to the pairs that are shared between them, and not between  $A_1$  (or  $A_2$ ) with the rest separately.

been proposed [15–18] culminating with the actual experimental measure in an ion-trap setting using shadow tomography [15, 16]. However, these moments are not direct indicators of the sign of the eigenvalues of  $\rho_A^{T_1}$  and hence of entanglement. Nevertheless, some linear combinations of them are sufficient conditions (known as  $p_n$ -PPT conditions, see below) for the presence of negative eigenvalues in the spectrum [15, 16] and so are witnesses of entanglement in mixed states. However, in contrast with the logarithmic negativity, for which a quasiparticle picture was derived in Ref. [19], results for the dynamics of the moments of the partial transpose are available only for Conformal Field Theories [20–22] (CFTs).

Here, by combining CFT and integrability, we derive the quasiparticle picture describing the dynamics of the moments of the partial transpose, and several related quantities, after a quantum quench in integrable systems. Specifically, we consider the Rényi negativities  $\mathcal{E}_n$  defined as

$$\mathcal{E}_n = \ln(\text{Tr}(\rho_A^{T_1})^n). \quad (1)$$

Note that  $\mathcal{E}_n$  are not proper entanglement measures, although the limit  $\lim_{n_e \rightarrow 1} \mathcal{E}_{n_e}$ , with  $n_e$  an even integer, defines the logarithmic negativity. We also consider the ratios  $R_n$  as

$$R_n = \frac{\text{Tr}(\rho_A^{T_1})^n}{\text{Tr}\rho_A^n}. \quad (2)$$

The ratios  $R_n$  are studied in CFT [23–27], due to their universality. Recently, they were studied at finite-temperature critical points [28], and to probe thermalization [29, 30] (note that the authors of Ref. [29] refer to the ratios  $R_n$  as Rényi negativities, unlike here). Here we derive the quasiparticle picture for both  $\mathcal{E}_n$  and  $R_n$ , focusing on the situation in which the subsystem  $A$  is made of two equal-length intervals at distance  $d$ . The formulas that we derive hold in the space-time scaling limit of  $t, \ell, d \rightarrow \infty$ , with the ratios  $t/\ell, d/\ell$  fixed. Furthermore, these results allow us to obtain predictions for all the  $p_n$ -PPT conditions introduced in Refs. [15, 16]. Interestingly, we argue that the ratios  $R_n$  in the space time scaling limit become proportional to the Rényi mutual information. Finally, we provide numerical benchmarks of our results for both free-fermion and free-boson models, although they are expected to hold for generic integrable systems.

The paper is organised as follows. In Sec. 2 we review the definitions of some entanglement measures, i.e. Rényi entropy, mutual information, Rényi negativity. In particular, in section 2.1 we introduce the moments of the partial transpose and the negativities. In section 2.2 we introduce the  $p_n$ -PPT conditions. In section 3 we review the CFT predictions for the out-of-equilibrium behavior of the Rényi negativities. Specifically, in section 3.1 we review the representation of the Rényi negativities in terms of twist fields. In section 3.2 we derive the out-of-equilibrium behavior of the Rényi negativities and the ratios  $R_n$  in CFTs. In Sec. 4 we introduce the quasiparticle picture (in section 4.1) for the spreading of entanglement and

negativity, generalizing it to the moments of the partial transpose in section 4.2. In section 5 we present numerical benchmarks for free bosonic (in section 5.1) and fermionic theories (in section 5.2). In section 5.3 we discuss the quasiparticle predictions for the  $p_n$ -PPT conditions. Finally, in section 6 we draw our conclusions and we discuss some possible extensions of our work.

## 2 Entanglement measures for mixed states

The Rényi entanglement entropies are the most successful way to characterize the bipartite entanglement of a subsystem  $A$  of a many-body quantum system prepared in a pure state (see e.g. the reviews [31–34]), also from the experimental perspective [7–10, 35, 36]. Given the reduced density matrix (RDM)  $\rho_A$  of a subsystem  $A$ , the Rényi entropies are defined as

$$S_A^{(n)} = \frac{1}{1-n} \ln \text{Tr} \rho_A^n. \quad (3)$$

From these, the von Neumann entropy is obtained as the limit  $n \rightarrow 1$  of Eq. (3) and also the entire spectrum of  $\rho_A$  can be reconstructed [37]. The Rényi entropies in Eq. (3) can be very conveniently computed in field theory because for integer  $n$ , in the path-integral formalism,  $\text{Tr} \rho_A^n$  is the partition function on an  $n$ -sheeted Riemann surface  $\mathcal{R}_n$  obtained by joining cyclically the  $n$  sheets along the region  $A$  [38–40].

For a mixed state, the entanglement entropies are no longer good measures of entanglement because they mix classical and quantum correlations (e.g. in a high temperature state,  $S_A^{(n)}$  gives the extensive result for the thermal entropy that has nothing to do with entanglement). In this respect, a useful quantity to consider is the Rényi mutual information

$$I_{A_1:A_2}^{(n)} \equiv S_{A_1}^{(n)} + S_{A_2}^{(n)} - S_{A_1 \cup A_2}^{(n)}, \quad (4)$$

which is not a measure of the entanglement between  $A_1$  and  $A_2$ , but for  $n \rightarrow 1$  it quantifies the amount of global correlations between the two subsystems (we mention that for  $n \neq 1$ ,  $I_{A_1:A_2}^{(n)}$  can be also negative [41] and a more complicated definition of mutual information must be employed [42]).

As anticipated, we are interested here in the entanglement between two different regions, and the goal of the following section is to define the tools to compute it.

### 2.1 Entanglement in mixed states and logarithmic negativity

A very useful starting point to quantify mixed state entanglement is the Peres criterion [11, 12], also known as PPT condition. It states that given a system described by the density matrix  $\rho_A$ , a sufficient condition for the presence of entanglement between two subsystems  $A_1$  and  $A_2$  (with  $A = A_1 \cup A_2$ ) is that the partial transpose  $\rho_A^{T_1}$  with respect to the degrees of freedom in  $A_1$  (or equivalently  $A_2$ ) has at least one negative eigenvalue. Let us introduce the partial transpose operation as follows. We can write down the density matrix as

$$\rho_A = \sum_{ijkl} \langle e_i^1, e_j^2 | \rho_A | e_k^1, e_l^2 \rangle | e_i^1, e_j^2 \rangle \langle e_k^1, e_l^2 |, \quad (5)$$

where  $|e_j^1\rangle$  and  $|e_k^2\rangle$  are orthonormal bases in the Hilbert spaces  $\mathcal{H}_1$  and  $\mathcal{H}_2$  corresponding to the  $A_1$  and  $A_2$  regions, respectively. The partial transpose of a density matrix for the subsystem  $A_1$  is defined by exchanging the matrix elements in the subsystem  $A_1$ , i.e.

$$\rho_A^{T_1} = \sum_{ijkl} \langle e_k^1, e_j^2 | \rho_A | e_i^1, e_l^2 \rangle | e_i^1, e_j^2 \rangle \langle e_k^1, e_l^2 |, \quad (6)$$

In terms of its eigenvalues  $\lambda_i$ , the trace norm of  $\rho_A^{T_1}$  can be written as

$$\mathrm{Tr}|\rho_A^{T_1}| = \sum_i |\lambda_i| = \sum_{\lambda_i > 0} |\lambda_i| + \sum_{\lambda_i < 0} |\lambda_i| = 1 + 2 \sum_{\lambda_i < 0} |\lambda_i|, \quad (7)$$

where in the last equality we used the normalisation  $\sum_i \lambda_i = 1$ . Here  $\mathrm{Tr}|O| \equiv \mathrm{Tr}\sqrt{O^\dagger O}$  denotes the trace norm of the operator  $O$ . This expression makes evident that the negativity measures “how much” the eigenvalues of the partial transpose of the density matrix are negative, a property which is the reason for the name negativity. Therefore, starting from the Peres criterion, a measure of the bipartite entanglement for a general mixed state can be naturally defined as [13]

$$\mathcal{E} \equiv \ln \mathrm{Tr}|\rho_A^{T_1}|, \quad (8)$$

which is known as *logarithmic negativity*. By considering the moments of the partial transpose RDM, one can define the Rényi negativities  $\mathcal{E}_n$  as

$$\mathcal{E}_n \equiv \ln \mathrm{Tr}(\rho_A^{T_1})^n. \quad (9)$$

The logarithmic negativity  $\mathcal{E}$  is given by the following replica limit [23, 24]

$$\mathcal{E} = \lim_{n_e \rightarrow 1} \mathcal{E}_{n_e}, \quad (10)$$

where  $n_e$  denotes an even number  $n_e = 2m$  with  $m$  integer. For future convenience, we also introduce the ratios

$$R_n \equiv \frac{\mathrm{Tr}(\rho_A^{T_1})^n}{\mathrm{Tr}\rho_A^n}. \quad (11)$$

The Rényi negativities  $\mathcal{E}_n$  with integer  $n \geq 2$  can also be measured in experiments [15, 17, 18], but they are not entanglement monotones. The entanglement negativity and Rényi negativities have been used to characterize mixed states in various quantum systems such as in harmonic oscillator chains [43–51], quantum spin models [25, 26, 52–63], (1+1)d conformal and integrable field theories [18, 23–27, 64–75], out-of-equilibrium settings [15, 19–21, 29, 30, 76–81].

Crucially, while for free-boson models the Rényi negativities for arbitrary real  $n$  can be efficiently computed from the two-point correlation function [43], this is not the case for free-fermion systems. The main problem is that the partial transpose in Eq. (8) is not a gaussian operator, although it can be written as the sum of two gaussian (non-commuting) operators  $O_\pm$  as [82]

$$\rho_A^{T_1} = \frac{1-i}{2}O_+ + \frac{1+i}{2}O_-. \quad (12)$$

From this observation a procedure to extract the Rényi negativities of integer order was proposed [82] and was also used in many subsequent studies [83–89]. Still, proceeding in this way, it is not possible to perform the replica limit  $n_e \rightarrow 1$ , implying that the negativity, i.e. the only genuine measure of entanglement, is not accessible. To overcome this problem, an alternative estimator of mixed-state entanglement for fermionic systems has been introduced based on the time-reversal partial transpose (a.k.a *partial time reversal*) [22, 90–96]. The new estimator has been dubbed *fermionic negativity*. It has been shown that the fermionic negativity is an entanglement monotone [92] and it is also an upper bound for the standard negativity. In the following, we denote  $\mathcal{E}_n^{(b)}$  the standard negativity in Eq. (9) (that is an entanglement monotone for both bosonic and fermionic systems) and  $\mathcal{E}_n^{(f)}$  the fermionic one (that exist only for fermionic models).  $\mathcal{E}^{(f)}$  reads as

$$\mathcal{E}^{(f)} = \ln \mathrm{Tr}\sqrt{O_+ O_-}, \quad (13)$$

with  $O_{\pm}$  as defined implicitly in Eq. (12). The (fermionic) Rényi negativities can be defined as [93]

$$\mathcal{E}_n^{(f)} = \begin{cases} \ln[\text{Tr}(O_+O_- \dots O_+O_-)], & n \text{ even,} \\ \ln[\text{Tr}(O_+O_- \dots O_+)], & n \text{ odd,} \end{cases} \quad (14)$$

from which  $\mathcal{E}^{(f)} = \lim_{n_e \rightarrow 1} \mathcal{E}_{n_e}^{(f)}$ . The products involving  $O_+$  and  $O_-$  are still gaussian fermionic operators, so all the above quantities can be efficiently computed, including the negativity (13).

## 2.2 Entanglement detection through partial transpose moments

Despite several sufficient conditions for entanglement in mixed states have been developed in the literature, many of them cannot be straightforwardly implemented experimentally since they require the knowledge of the full density matrix [31]. This is for instance the case of the PPT condition. To overcome this difficulty, it was shown in [15] that the first few moments of the partial transpose can be used to define some simple yet powerful tests for bipartite entanglement. Given  $\rho_A^{T_1}$  (cf. Eq. (6)), we denote its  $k$ -th order moment as

$$p_k \equiv \text{Tr}(\rho_A^{T_1})^k, \quad (15)$$

with  $p_1 = \text{Tr}(\rho_A^{T_1}) = 1$  and  $p_2$  equal to the purity  $p_2 = \text{Tr}\rho_A^2$ . The  $p_3$ -PPT condition states that any positive semi-definite partial transpose satisfies [15]

$$p_3 p_1 > p_2^2, \quad (16)$$

or, in other words, if  $p_3 < p_2^2$ , then  $\rho_A$  violates the PPT condition and must therefore be entangled. The condition in Eq. (16) belongs to a more general set of conditions, dubbed Stieltjes $_n$ , involving inequalities among the moments  $p_k$  of order up to  $n$ . They were introduced in [16] together with a set of experimentally accessible conditions for detecting entanglement in mixed states. The condition Stieltjes $_3$  is equivalent to  $p_3$ -PPT, and so we rename here the Stieltjes $_n$ -conditions as  $p_n$ -PPT. As examples,  $p_5$ -PPT and  $p_7$ -PPT read, respectively [16]

$$D_5 \equiv \det \begin{pmatrix} p_1 & p_2 & p_3 \\ p_2 & p_3 & p_4 \\ p_3 & p_4 & p_5 \end{pmatrix} \geq 0, \quad D_7 \equiv \det \begin{pmatrix} p_1 & p_2 & p_3 & p_4 \\ p_2 & p_3 & p_4 & p_5 \\ p_3 & p_4 & p_5 & p_6 \\ p_4 & p_5 & p_6 & p_7 \end{pmatrix} \geq 0, \quad (17)$$

from which one deduces easily the rationale for higher order condition.

## 3 Quench dynamics of Rényi negativities in conformal field theory

In this section we review the CFT calculation of the temporal evolution of the Rényi negativities between two intervals after a global quench in CFT as derived in Ref. [20]. We consider  $A = A_1 \cup A_2$ , where the intervals  $A_1$  and  $A_2$  can be either adjacent or disjoint (see Fig. 1).

### 3.1 Rényi negativities from twist field correlation functions

A powerful method to calculate the Rényi negativities is based on a particular type of twist fields in quantum field theory that are related to branch points in the Riemann surface  $\mathcal{R}_n$  [40,97]. We denote twist and anti-twist fields by  $\mathcal{T}_n$  and  $\tilde{\mathcal{T}}_n$ , respectively. One can show that the moments

of the reduced density matrix  $\text{Tr}(\rho_A)^n$  can be written as correlators of twist fields [40]. For example, when  $A = [u_1, u_2] \cup [u_3, u_4]$  (see Fig. 1), one has that

$$\text{Tr}\rho_A^n = \langle \mathcal{T}_n(u_1)\tilde{\mathcal{T}}_n(u_2)\mathcal{T}_n(u_2)\tilde{\mathcal{T}}_n(u_3) \rangle. \quad (18)$$

Notice that the twist and anti-twist fields are inserted at the endpoints of  $A$ . The expectation value in Eq. (18) is taken with respect to the action living on a plane. As shown in [24], if we take the partial transpose  $\rho_A^{T_1}$  with respect to the degrees of freedom living on the interval  $A_1 = [u_1, v_1]$ ,  $\text{Tr}(\rho_A^{T_1})^n$  can be written as a twist-field correlator as in Eq. (18), the only difference being that the twist fields  $\mathcal{T}_n$  and  $\tilde{\mathcal{T}}_n$  at the endpoints of  $A_1$  are exchanged while the remaining ones stay untouched, i.e. [23, 24]

$$\text{Tr}(\rho_A^{T_1})^n = \langle \tilde{\mathcal{T}}_n(u_1)\mathcal{T}_n(u_2)\mathcal{T}_n(u_3)\tilde{\mathcal{T}}_n(u_4) \rangle. \quad (19)$$

This procedure can be generalized straightforwardly to the case where  $A$  is the union of more than two intervals, and the partial transposition involves more than two intervals.

The situation in which the two intervals are adjacent can be obtained from Eq. (19) by taking the limit  $u_3 \rightarrow u_2$  in Eq. (19), giving  $\text{Tr}(\rho_A^{T_1})^n = \langle \tilde{\mathcal{T}}_n(u_1)\mathcal{T}_n^2(u_2)\tilde{\mathcal{T}}_n(u_4) \rangle$ . In a generic CFT characterized by a central charge  $c$ , the expectation values (18) and (19) are evaluated straightforwardly by knowing the scaling dimensions of  $\mathcal{T}_n, \tilde{\mathcal{T}}_n, \mathcal{T}_n^2$  and  $\tilde{\mathcal{T}}_n^2$ . The scaling dimensions of  $\mathcal{T}_n^2$  and  $\tilde{\mathcal{T}}_n^2$  are equal, and depend on the parity of  $n$  as [23]

$$\Delta_n^{(2)} \equiv \begin{cases} \Delta_n & \text{odd } n \\ 2\Delta_{n/2} & \text{even } n \end{cases}, \quad \Delta_n = \frac{c}{12} \left( n - \frac{1}{n} \right), \quad (20)$$

where  $\Delta_n$  are the scaling dimensions of  $\mathcal{T}_n, \tilde{\mathcal{T}}_n$ .

### 3.2 Out-of-equilibrium dynamics of the Rényi negativities

Before discussing the out-of-equilibrium dynamics after a quantum quench of the Rényi negativities in CFTs, it is useful to recall the imaginary time formalism for the description of quantum quenches [1–3]. The family of initial states that are easy to work with in CFT have the form  $e^{-\tau_0 H}|\psi_0\rangle$ , with  $|\psi_0\rangle$  being a boundary state. The expectation value of a local operator  $O$  is then

$$\langle O(t, x) \rangle = Z^{-1} \langle \psi_0 | e^{iHt - \tau_0 H} O(x) e^{-iHt - \tau_0 H} | \psi_0 \rangle, \quad (21)$$

where the damping factors  $e^{-\tau_0 H}$  have been introduced to make the path integral absolutely convergent (see below), and  $Z = \langle \psi_0 | e^{-2\tau_0 H} | \psi_0 \rangle$  is the normalisation factor. The correlator in Eq. (21) may be represented by a path integral in imaginary time  $\tau$  as [2]

$$\langle O(t, x) \rangle = Z^{-1} \int [d\varphi(x, \tau)] O(x, \tau = \tau_0 + it) e^{-\int_{\tau_1}^{\tau_2} L d\tau} \langle \psi_0 | \phi(x, \tau_2) \rangle \langle \phi(x, \tau_1) | \psi_0 \rangle, \quad (22)$$

where  $L$  is the (euclidean) Lagrangian corresponding to the dynamics induced by  $H$ ,  $\tau_1$  can be identified with 0 and  $\tau_2$  with  $2\tau_0$ . As shown in [1, 3], the computation of the path integral in Eq. (22) can be done considering  $\tau$  real and only at the end analytically continuing it to the complex value  $\tau = \tau_0 + it$ .

In this way, the problem of the dynamics is mapped to the thermodynamics of a field theory in a strip geometry of width  $2\tau_0$  and boundary condition  $|\psi_0\rangle$  at the two edges of the strip in the imaginary time direction. At this point we have all the ingredients to derive the dynamics of the Rényi negativities after a global quench in CFT. To calculate the time-dependent  $\text{Tr}(\rho_A^{T_1})^n$  one has to compute the correlator

$$\text{Tr}(\rho_A^{T_1})^n = \langle \tilde{\mathcal{T}}_n(\omega_1)\mathcal{T}_n(\omega_2)\mathcal{T}_n(\omega_3)\tilde{\mathcal{T}}_n(\omega_4) \rangle, \quad (23)$$

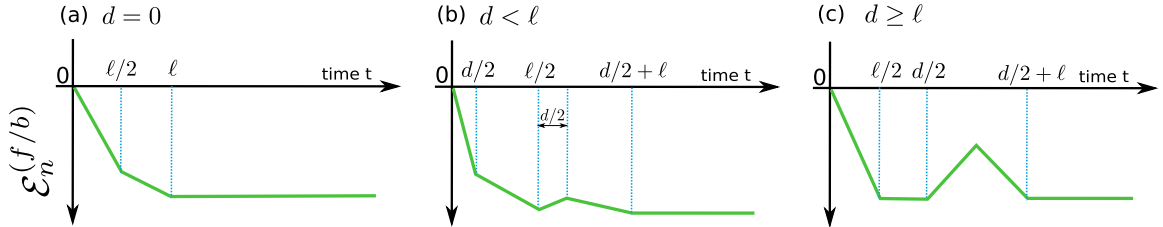


**Figure 2:** Time dependence of the Rényi negativities for quasiparticles with linear dispersion. We consider two disjoint subsystems with equal length  $\ell$  at distance  $d = 0$  (a),  $d < \ell$  (b),  $d \geq \ell$  (c). The piece-wise linear behavior is described by Eq. (24).

where the expectation value has to be calculated in the field theory confined in a strip, and where we denoted by  $\omega_i = u_i + i\tau$  the complex coordinate on the strip ( $u_i \in \mathbb{R}$  and  $0 < \tau < 2\tau_0$ ). It is convenient to employ the conformal transformation  $z = e^{\pi\omega/(2\tau_0)}$ , which maps the strip onto the half plane, where the four point correlation functions of the twist fields can be computed by knowing that they behave as primary fields with scaling dimensions  $\Delta_n$  (cf. (20)). After the analytic continuation to real time, in the space-time scaling limit  $t, |u_i - u_j| \gg \tau_0$ , from Eq. (23), the Rényi negativities  $\mathcal{E}_n$  (cf. Eq. (9)) read [20]

$$\begin{aligned} \mathcal{E}_n = & -\frac{\pi}{\tau_0} \left[ 2\Delta_n t + \Delta_n \left( \frac{\ell_1 + \ell_2}{2} - \max(t, \ell_1/2) - \max(t, \ell_2/2) \right) + (\Delta_n^{(2)}/2 - \Delta_n) \right. \\ & \left. \times (\max(t, (\ell_1 + \ell_2 + d)/2) + \max(t, d/2)) - \max(t, (\ell_1 + d)/2) - \max(t, (\ell_2 + d)/2) \right], \quad (24) \end{aligned}$$

where  $\Delta_n^{(2)}$  is in Eq. (20), and we defined  $\ell_1 = |u_1 - u_2|$ ,  $\ell_2 = |u_3 - u_4|$ , and  $d = |u_3 - u_2|$  (see Fig. 1). In deriving Eq. (24) we neglected an additive time-independent constant that originates from the correlation function of the twist fields, and that depends on the details of the CFT under consideration. This is justified because Eq. (24) holds in the scaling limit  $\ell_1, \ell_2, d, t \rightarrow \infty$  with their ratios fixed, and it describes only the leading behavior of the Rényi negativities  $\mathcal{E}_n$  in that limit. Crucially, Eq. (24) depends on both  $\Delta_n$  and  $\Delta_n^{(2)}$ . Notice that even for finite  $d$ ,  $\mathcal{E}_n$  exhibits a linear behavior at short times, due to the first term in Eq. (24). This signals that  $\mathcal{E}_n$  are not good measures of the entanglement or the correlation between  $A_1$  and  $A_2$ . The reason is that for  $t \ll d$  no correlation can be shared between  $A_1$  and  $A_2$  because the maximum velocity in the system is finite (see Fig. 2). We stress that Eq. (24) is not directly applicable to microscopic integrable models: Eq. (24) is only valid for CFT, in which there is a perfect linear dispersion, i.e., only one velocity. This is not the case in integrable lattice models, where the excitations have a nonlinear dispersion. In the next sections, we will show how to adapt Eq. (24) to describe the dynamics of the Rényi negativities after a quantum quench in microscopic integrable systems.

Finally, the dynamics of the ratio  $R_n$  in Eq. (11) can be derived combining Eq. (24) with the results for  $\text{Tr}\rho_A^n$  in [3]. The final result reads [20]

$$\begin{aligned} \ln R_n = & \frac{\pi\Delta_n^{(2)}}{\tau_0} \\ & \times (-\max(t, (\ell_1 + \ell_2 + d)/2) - \max(t, d/2)) + \max(t, (\ell_1 + d)/2) + \max(t, (\ell_2 + d)/2). \quad (25) \end{aligned}$$

In contrast with Eq. (24), Eq. (25) does not depend explicitly on  $\Delta_n$ , but only on  $\Delta_n^{(2)}$ .

Before concluding, it is useful to discuss the qualitative behavior of  $\mathcal{E}_n^{(f/b)}$  and  $-\ln(R_n^{(f/b)})$ . The typical behavior of the Rényi negativities, as obtained from Eq. (24), is reported in Fig. 2 for three typical values of the distance  $d$  between the two intervals of equal length  $\ell$ .  $\mathcal{E}_n$  is always a piecewise linear function and it is negative at any time. For  $d = 0$  one has a two-slope linear behavior followed by a saturation to a volume-law scaling at long times. At intermediate



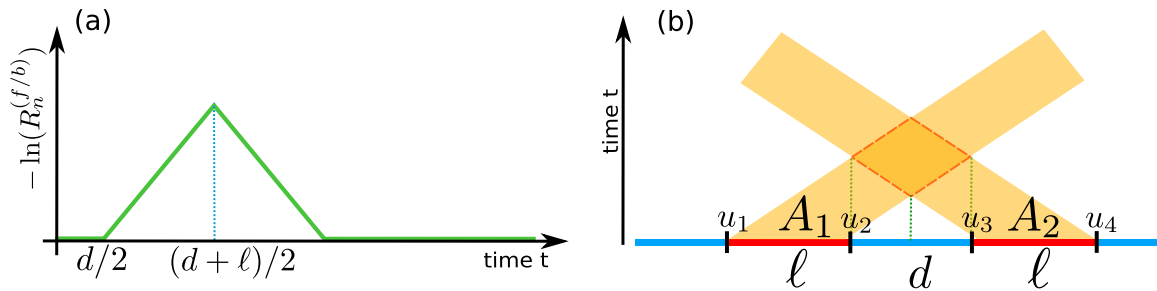


**Figure 3:** Illustration of the dynamics of  $-\ln R_n^{(f/b)}$  for two disjoint subsystems with equal length  $\ell$  at distance  $d$ . On the left we report the shape of  $-\ln R_n^{(f/b)}$  with a single velocity of quasiparticles. On the right, there is a graphical representation for the quasi-particle spreading of entanglement (for the case with all quasi-particles having the same velocity  $v = 1$  as in a CFT). Horizontal slices of the dark orange region count the quasiparticles shared between the two disjoint sets at a given time.

distance  $0 < d < \ell$  the behavior is more complicated with a change in the sign of the slope. For  $d > \ell$ ,  $\mathcal{E}_n^{(f/b)}$  exhibits an initial linear decrease followed by a saturation, and a dip-like feature at  $d/2 \leq t \leq d/2 + \ell$ .

The dynamics of  $-\ln(R_n^{(f/b)})$  (cf. Eq. (25)) is shown in Fig. 3 for two equal-length intervals. For  $t < d/2$ , it vanishes; for  $d/2 \leq t \leq (d + \ell)/2$  it linearly increases, then it linearly decreases with the same (in absolute value) slope until  $t \leq (d + 2\ell)/2$ , when it vanishes and stays zero for all larger times. Therefore, at a given time  $t$ , it is proportional to the width of the intersection between the two shaded areas starting from  $A_1 \cup A_2$  and showed in Fig. 3 (b). In other words, it is proportional to the total number of entangled pairs shared between  $A_1$  and  $A_2$ . This property suggests that in the scaling limit,  $R_n$  becomes an indicator of the mutual entanglement between the intervals, although in general it is not an entanglement monotone.

Let us remark that Eq. (25) is identical to the evolution of the Rényi mutual information in Eq. (4) apart from the prefactor. We will come back to the connection between these two quantities in the following sections.

## 4 Quasiparticle picture for the Rényi negativities in integrable systems

The goal of this section is to adapt Eq. (24) and Eq. (25) to describe the dynamics of the Rényi negativities and the ratios  $R_n$  after a quantum quench in integrable systems. The main observation is that Eq. (24) and Eq. (25) admit an interpretation in terms of a simple hydrodynamic picture, a.k.a. the quasiparticle picture.

### 4.1 Quasiparticle picture

The quasiparticle picture for the entanglement dynamics after a global quantum quench has been proposed in Ref. [3]. The underlying idea is that the pre-quench initial state has very high energy with respect to the ground state of the Hamiltonian governing the dynamics; hence it can be seen as a source of quasiparticle excitations at  $t = 0$ . We assume that quasiparticles are uniformly created in uncorrelated pairs with quasimomenta  $(k, -k)$  and traveling with opposite velocities  $v(k) = -v(-k)$  (for free models the uncorrelated pair assumption can be released, see [98–101]; for interacting integrable models it has been argued that the pair structure is what makes the quench integrable [102]). Quasiparticles produced at the same point in space are entangled, whereas quasiparticles created far apart are incoherent. The quasiparticles travel through the system as free-like excitations. At a generic time  $t$ , the von Neumann entropy and

the Rényi entropies between a subsystem  $A$  and the rest is proportional to the total number of quasiparticles that were created at the same point at  $t = 0$  and are shared between  $A$  and its complement at time  $t$  (see Fig. 2 (a)). Let us focus on the quasiparticle picture for the Rényi entropies in free models (the quasiparticle picture has been derived rigorously for free-fermion models in Ref. [103]). In formulas it reads as

$$S_A^{(n)}(t) = \int \frac{dk}{2\pi} s_{GGE}^{(n)}(k) \min(2|v(k)|t, \ell). \quad (26)$$

Here  $\ell$  is the length of subsystem  $A$ , and  $v(k)$  is the group velocity of the fermionic excitations. Importantly, in Eq. (26)  $s_{GGE}^{(n)}(k)$  is the density (in momentum space) of the Rényi entropies of the GGE thermodynamic state [104–106] that describes the steady state after the quench. Eq. (26) predicts a linear growth for  $t \leq \ell/(2v_{\max})$ , with  $v_{\max} \equiv \max_k(v(k))$  the maximum velocity in the system, and then saturates to an extensive value at  $t \rightarrow \infty$ .

For  $n = 1$ , i.e., for the von Neumann entropy the validity of Eq. (26) for a generic interacting integrable model has been conjectured in Ref. [4, 5]. Eq. (26) remains essentially the same. Precisely, the contribution of the quasiparticles to the von Neumann entropy  $s_{GGE}^{(1)}$  is the density of GGE thermodynamic entropy. The group velocities of the quasiparticles are obtained as particle-hole excitations over the GGE thermodynamic macrostate [5, 107]. This conjecture has been explicitly worked out in several cases [4, 5, 108, 109] and tested against numerics in several interacting integrable models. [4, 5, 110, 111] Eq. (26) has been generalized to describe the steady-state value of the Rényi entropies [112–114]. On the other hand, the full-time dynamics of the Rényi entropies is still an open problem, with the exception of one model [115, 116]. Eq. (26) can be straightforwardly generalized to describe the dynamics of the mutual information between two intervals. This allows to reveal how quantum information is scrambled in integrable systems [117, 118]. Remarkably, the quasiparticle picture for the logarithmic negativity has been derived in Ref. [66]. By combining the quasiparticle picture with the framework of the Generalized Hydrodynamics [119, 120] it is possible to describe the entanglement dynamics after quenches from inhomogeneous initial states [121–126]. The quasiparticle picture for the entanglement dynamics has been also tested in the rule 54 chain, which is believed to be a representative “toy model” for generic interacting integrable systems [115, 116]. Very recently, the quasiparticle picture has been generalized to take into account dissipative effects, at least in free-fermion and free-boson models [127–130], to describe the evolution of the symmetry-resolved entanglement entropies [131, 132], and for the characterization of the prethermalization dynamics [133].

To proceed it is useful to compare Eq. (26) with the CFT prediction for the dynamics of the Rényi entropies [3]

$$S_A^{(n)} = -\frac{1}{1-n} \frac{\pi \Delta_n}{2\tau_0} \min(2t, \ell). \quad (27)$$

A crucial observation is that Eq. (26) can be formally obtained from the CFT result in Eq. (27) by replacing  $t \rightarrow |v(k)|t$ , integrating over the quasiparticles with quasimomentum  $k$ , and replacing  $-\pi \Delta_n/(2\tau_0) \rightarrow s_{GGE}^{(n)}$ .

## 4.2 The quasiparticle description for Rényi negativities

The quasiparticle picture described above can be adapted to describe the Rényi negativities  $\mathcal{E}_n^{(f/b)}$  and the ratios  $\ln(R_n^{(f/b)})$ , in integrable systems after a global quench.

Indeed, similarly to the Rényi entropies, from Eqs. (24) and (25), by using Eq. (20), after

replacing  $-\pi\Delta_n/(2\tau_0) \rightarrow s_{GGE}^{(n)}$ , and by integrating over  $k$ , one obtains that

$$\begin{aligned} \mathcal{E}_n^{(f/b)} = \int \frac{dk}{2\pi} & \left[ 4\varepsilon_n |v|t + 2\varepsilon_n \left( \frac{\ell_1 + \ell_2}{2} - \max(|v|t, \ell_1/2) - \max(|v|t, \ell_2/2) \right) \right. \\ & - (2\varepsilon_n - \varepsilon_n^{(2)}) (\max(|v|t, (\ell_1 + \ell_2 + d)/2) + \max(|v|t, d/2) \\ & \left. - \max(|v|t, (\ell_1 + d)/2) - \max(|v|t, (d + \ell_2)/2) \right), \end{aligned} \quad (28)$$

while the ratios  $R_n^{(f/b)}$  read

$$\begin{aligned} \ln(R_n^{(f/b)}) = \int \frac{dk}{2\pi} \varepsilon_n^{(2)} & (\max(|v|t, d/2) - \max(|v|t, (\ell_1 + d)/2) \\ & - \max(|v|t, (\ell_2 + d)/2) + \max(|v|t, (\ell_1 + \ell_2 + d)/2)). \end{aligned} \quad (29)$$

We defined

$$\varepsilon_n^{(2)}(k) \equiv \begin{cases} \varepsilon_n(k) & \text{odd } n \\ 2\varepsilon_{n/2}(k) & \text{even } n \end{cases}, \quad \varepsilon_n(k) = s_{GGE}^{(n)}(k). \quad (30)$$

Clearly, Eq. (30) mirrors the structure of Eq. (20). Here  $s_{GGE}(k)$  is the density of  $GGE$  thermodynamic entropy.

It is interesting to remark that by comparing Eq. (29) with the quasiparticle picture for the Rényi mutual informations [5]  $I_{A_1:A_2}^{(n)}$ , one obtains

$$\ln(R_n^{(f/b)}) = \begin{cases} (1-n)I_{A_1:A_2}^{(n/2)} & n \text{ even} \\ (1-n)\frac{I_{A_1:A_2}^{(n)}}{2}, & n \text{ odd.} \end{cases} \quad (31)$$

Moreover, by taking the replica limit  $n_e \rightarrow 1$  in  $\mathcal{E}_{n_e}^{(f/b)}$ , we recover the quasiparticle prediction for the negativity [19]

$$\begin{aligned} \mathcal{E}^{(f/b)} = \int \frac{dk}{2\pi} \varepsilon_{1/2}(k) & (\max(2|v|t, d) - \max(2|v|t, \ell_1 + d) \\ & - \max(2|v|t, \ell_2 + d) + \max(2|v|t, \ell_1 + \ell_2 + d)). \end{aligned} \quad (32)$$

It was pointed out in [19] that Eq. (32) is the same as for the Rényi mutual information (of any index) by replacing  $\varepsilon_{1/2}$  with the density of Rényi entropy. We stress that the same prediction is valid for both standard (bosonic) partial transpose and for the fermionic one.

Finally, it is useful to observe that Eq. (31) can be derived by using that if  $A_1 \cup A_2$  is in a pure state then  $\text{Tr}((\rho_A^{T_1})^n)$  can be expressed in terms of  $\text{Tr}(\rho_{A_1}^n)$ . More precisely, one can prove that [24]

$$\text{Tr}(\rho_A^{T_1})^n = \begin{cases} \text{Tr}\rho_{A_1}^n & n \text{ odd} \\ (\text{Tr}\rho_{A_1}^{n/2})^2 & n \text{ even} \end{cases} \quad (33)$$

where  $\rho_{A_1} = \text{Tr}_{A_2}\rho_A$ . Now, one can recover Eq. (31) by using Eq. (33), and the definition in Eq. (4), and that if  $A_1 \cup A_2$  is in a pure state,  $S_{A_1}^{(n)} = S_{A_2}^{(n)}$ . The fact that the result of the quasiparticle picture (24) is not sensitive to  $A_1 \cup A_2$  not being in a pure state reflects that the initial state has low entanglement and that during the dynamics the entanglement is transported ballistically.

Finally, for Eq. (28) and Eq. (29) to be predictive one has to fix the function  $s_{GGE}(k)$  (cf. Eq. (30)). Here we focus on out-of-equilibrium protocols for free-fermion and free-boson models.

In this situation,  $s_{GGE}(k)$  is determined from the population of the modes  $\rho(k)$  of the postquench Hamiltonian in the stationary state (see Refs. [6, 134] for a pedagogical review). Actually, since  $\rho(k)$  are conserved they can be equivalently computed in the initial state, without solving the dynamics. Specifically, one has that

$$s_{GGE}^{(n,f/b)}(k) = \pm \ln(\pm \rho(k)^n + (1 \mp \rho(k))^n), \quad (34)$$

where the upper and lower signs are for fermionic and bosonic systems, respectively (and not to fermionic and bosonic negativity). We remark that, although the quasiparticle prediction in Eqs. (28) and (29) is expected to be valid also for interacting integrable models, the full quasiparticle picture for the Rényi entropies is not known.

## 5 Time evolution of Rényi negativities in free models: Numerical results

In this section we provide numerical benchmarks for the results of section 4.2. As an example of free-bosonic system, we consider the harmonic chain. Our results for free-fermion systems are tested against exact numerical data for a fermionic chain.

### 5.1 Mass quench in the harmonic chain

Let us start discussing the dynamics of the Rényi negativities after a mass quench in the harmonic chain. The harmonic chain is described by the Hamiltonian

$$H = \frac{1}{2} \sum_{n=0}^{L-1} p_n^2 + m^2 q_n^2 + (q_{n+1} - q_n)^2, \quad q_0 = q_L, p_0 = p_L, \quad (35)$$

where  $L$  is the number of lattice sites,  $q_n$  and  $p_n$  are canonically conjugated variables, with  $[q_n, p_m] = i\delta_{nm}$ , and  $m$  is a mass parameter. The harmonic chain can be diagonalized in Fourier space and is equivalent to a system of free bosons. The dispersion relation of the bosons is given by [6]

$$e(k) = [m^2 + 2(1 - \cos(k))]^{1/2}. \quad (36)$$

The group velocities are obtained from the single particle energies  $e(k)$  as

$$v(k) = \frac{de(k)}{dk} = \sin(k)[m^2 + 2(1 - \cos(k))]^{-1/2}, \quad (37)$$

and the maximum one is  $v_{\max} = \max_k v(k)$ . In the mass quench protocol, the system is prepared in the ground state  $|\psi_0\rangle$  of the Hamiltonian (35) with  $m = m_0$ . At  $t = 0$  the mass parameter is quenched from  $m_0$  to a different value  $m$  and the system unitarily evolves under the new Hamiltonian  $H(m)$ , namely  $|\psi(t)\rangle = e^{-iHt} |\psi_0\rangle$ . The density  $\rho(k)$  (cf. Eq. (34)) of the bosons is written in terms of the pre- and post-quench dispersions  $e_0(k)$  and  $e(k)$  as [2, 3, 6]

$$\rho(k) = \frac{1}{4} \left( \frac{e(k)}{e_0(k)} + \frac{e_0(k)}{e(k)} \right) - \frac{1}{2}. \quad (38)$$

For free bosonic systems the Rényi negativities can be constructed from the two-point correlation functions  $\langle q_i q_j \rangle$ ,  $\langle p_i p_j \rangle$  and  $\langle q_i p_j \rangle$ . Indeed, given a subsystem  $A$  containing  $\tilde{\ell}$  sites, which could be either all in one interval or in disjoint intervals, the reduced density matrix for  $A$  can be studied [20, 135] by constructing the  $\tilde{\ell} \times \tilde{\ell}$  matrices  $Q_{ij}^A = \langle q_i q_j \rangle$ ,  $P_{ij}^A = \langle p_i p_j \rangle$  and  $R_{ij}^A = \text{Re} \langle q_i p_j \rangle$ , where the superscript  $A$  means that the indices  $i, j$  are restricted to subsystem  $A$ . Crucially, a similar strategy can be used to construct the Rényi negativities (for the details we refer to

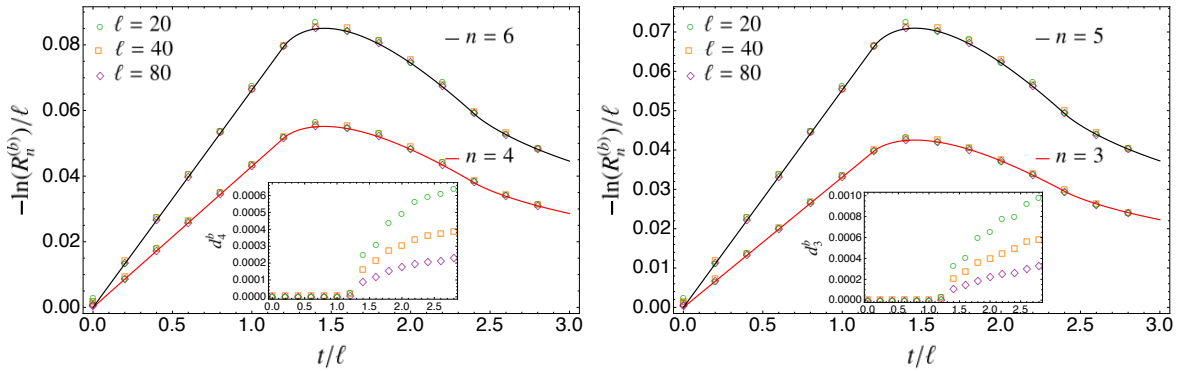


**Figure 4:** Logarithms of the moments of the (bosonic) partial transpose after the mass quench from  $m_0 = 1$  to  $m = 2$  in the harmonic chain. The quantity  $-\ln(R_n^{(b)})/\ell$  is plotted versus rescaled time  $t/\ell$ , with  $\ell$  the intervals' length. The analytical predictions represented by continuous lines correspond to Eq. (29). The insets represent Eq. (39) and they prove the validity of Eq. (31), i.e. the connection between the ratio  $R_n$  and the Rényi mutual information.

Ref. [20]). The main idea is that the net effect of the partial transposition with respect to a subinterval  $A_1$  is the inversion of the signs of the momenta corresponding to the sites belonging to  $A_1$ .

For the following, we restrict ourselves to the physical situation with  $A$  made of two disjoint parts, i.e.,  $A = A_1 \cup A_2$ , with  $A_1, A_2$  two equal-length intervals of length  $\ell$ . We denote as  $d$  the distance between  $A_1$  and  $A_2$  (see Fig. 1). We only discuss the ratios  $-\ln(R_n^{(b)})$  (cf. Eq. (11)). The results are shown in Fig. 4. Panels (a) and (b) show the quantities  $-\ln(R_n^{(b)})/\ell$  for adjacent intervals, i.e.,  $d = 0$ . The data are for several values of the intervals' length  $\ell$  up to  $\ell \leq 80$ . Since we are interested in the scaling limit, we plot  $-\ln(R_n^{(b)})/\ell$  versus the rescaled time  $t/\ell$ . For two adjacent intervals, the ratio exhibits a linear growth for  $t/\ell \sim 1.25$ , which reflects the maximum velocity being  $v_{\max} \sim 0.4$ . For larger times we observe a slow decrease toward zero for  $t/\ell \rightarrow \infty$ . This slow decay is due to the slower quasiparticles with  $v < v_{\max}$ . The solid line is the theoretical prediction in Eq. (29). At finite  $\ell$  and  $t$  the data exhibit some small corrections from Eq. (29), which is recovered in the scaling limit  $t, \ell \rightarrow \infty$  with their ratio fixed.

It is also useful to investigate directly the validity of Eq. (31), which establishes a relationship between  $R_n^{(f/b)}$  and the mutual information. To this aim, we introduce the difference  $d_n^{(f/b)}$  as

$$d_n^{(f/b)} = \begin{cases} \ln(R_n^{(f/b)}) - (1-n)I_{A_1:A_2}^{(n/2)} & n \text{ even} \\ \ln(R_n^{(f/b)}) - (1-n)\frac{I_{A_1:A_2}^{(n)}}{2}, & n \text{ odd} \end{cases} \quad (39)$$

As it is clear from the insets in Fig. 4,  $d_n^{(b)}$  is very small in the region of linear growth, i.e., for  $2v_{\max}t/\ell \leq 1$  (an obvious fact, since in the scaling limit it is just  $0 - 0$ ). At fixed  $\ell$ , in the non-trivial region, i.e. for larger values of the scaling variable  $2v_{\max}t/\ell$ ,  $d_n^{(b)}$  is larger. However, at fixed  $t/\ell$ , the deviations  $d_n^{(b)}$  decrease with increasing  $\ell$ , and in the scaling limit  $\ell \rightarrow \infty$  one recovers Eq. (31). Precisely, the data suggest a behavior  $d_n^{(b)} \propto 1/\ell$ .

## 5.2 Quench in a free fermion chain

We now discuss numerical results for free-fermion systems described by the Hamiltonian

$$H = \sum_{j=1}^L \left( \frac{1}{2} [c_j^\dagger c_{j+1}^\dagger + c_{j+1} c_j + c_j^\dagger c_{j+1} + c_{j+1}^\dagger c_j] - hc_j^\dagger c_j \right), \quad (40)$$

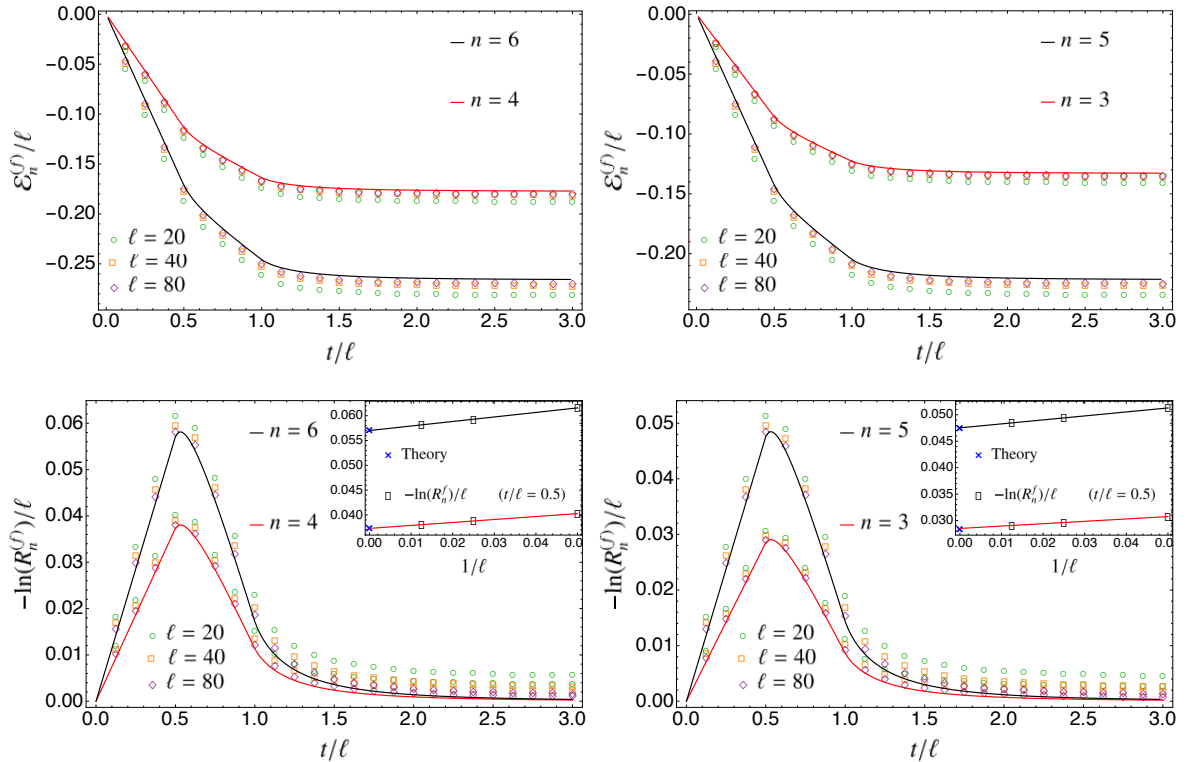


**Figure 5:** Logarithms of the moments of the (fermionic) partial transpose after a quench in the fermionic chain (with  $h_0 = 10$  and  $h = 2$ ) for two adjacent intervals. Both  $-\ln(R_n^{(f)})/\ell$  and  $\mathcal{E}_n^{(f)}/\ell$  are plotted versus rescaled time  $t/\ell$ , with  $\ell$  the intervals' length. The analytical predictions represented by continuous lines correspond to Eq. (28) (top panels) and (29) (bottom panels). The insets investigate the finite-size scaling corrections: the symbols are for the fermionic negativity at fixed  $t/\ell = 0.5$ ; the crosses are the theoretical results in the thermodynamic limit; the solid lines are linear fits.

where  $\{c_i, c_j^\dagger\} = \delta_{ij}$  are anti-commuting fermionic operators,  $h$  is a coupling parameter, e.g. a magnetic field, and we neglect boundary terms (we are interested in the thermodynamic limit  $L \rightarrow \infty$ ). A Jordan-Wigner transformation maps the Hamiltonian to the well-known transverse field Ising chain. However, the spin RDM is not simply mapped to the fermion RDM for two disjoint intervals [136, 137]. Instead, for the case of adjacent intervals they are mapped into each other and so the following results for fermions apply also to the spin variables.

In terms of the momentum space Bogoliubov fermions the Hamiltonian is diagonal and the single-particle energies are

$$e(k) = [h^2 - 2h \cos(k) + 1]^{1/2}. \quad (41)$$

We consider the non-equilibrium unitary dynamics that follows from a quench of the field  $h$  at  $t = 0$  from  $h_0$  to  $h \neq h_0$ . In order to parametrise the quench it is useful to introduce the angle  $\Delta(k)$  as [2]

$$\cos(\Delta(k)) = \frac{1 + hh_0 - (h + h_0) \cos(k)}{e(k)e_0(k)}. \quad (42)$$

As for free-bosons, the central object to obtain the quasiparticle prediction is the density  $\rho(k)$  of the Bogoliubov fermions. This is given by [138, 139]

$$\rho(k) = \frac{1}{2}(1 - \cos(\Delta(k))). \quad (43)$$

The reduced density matrix can be completely characterized [135] by the two-point correlation functions restricted to the subsystem  $A$ . From the covariance matrix associated to  $\rho_A$ , one can

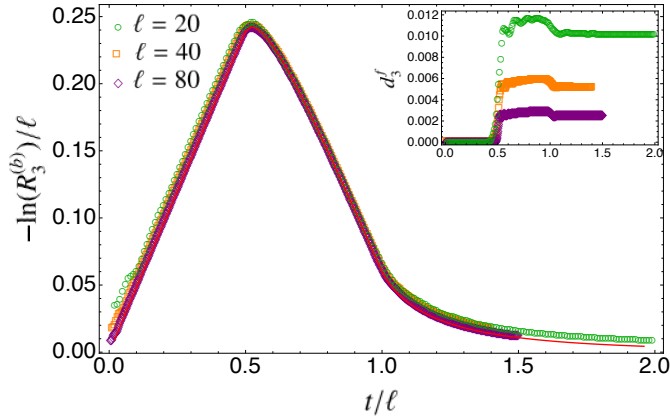


**Figure 6:** Standard Rényi negativity for  $n = 3$  after a quench in the free fermion chain (with  $h_0 = 0.1$  and  $h = 2$ ). The numerical data (symbols) have been obtained by expanding the third power of  $\rho_A^{T_1}$  as in Eq. (44) while the solid red line correspond to Eq. (29). The inset represent Eq. (39) and it proves the validity of Eq. (31) in the space-time scaling limit.

build the covariance matrix corresponding to the partial time reversal  $\rho_A^{R_1}$  (see Ref. [90–95]). The fermionic Rényi negativities  $\mathcal{E}_n^{(f)}$  introduced in Eq. (14) can be efficiently computed in terms of the eigenvalues of the covariance matrix.

We discuss the numerical results for both  $\mathcal{E}_n^{(f)}$  and  $R_n^{(f)}$  for two adjacent intervals in Fig. 5, for the quench with  $h_0 = 10$  and  $h = 2$ . We first discuss the Rényi negativities  $\mathcal{E}_n^{(f)}$  in Fig. 4 (top) plotting  $\mathcal{E}_n^{(f)}/\ell$  versus  $t/\ell$ . We consider only the geometry with two adjacent intervals. The numerical data exhibit the expected behavior as in Fig. (2) (a). One has  $\mathcal{E}_n^{(f)} \leq 0$  at all times. The negativities exhibit a two-slope decrease at short times, which is followed by a saturation at long times. In contrast with the CFT case, the saturation is not abrupt due to the fact that the quasiparticles have a nontrivial dispersion. The different symbols in the figure denote different subsystem size  $\ell$ . In the thermodynamic limit  $\ell \rightarrow \infty$  the numerical data approach the prediction of the quasiparticle picture (continuous line in the figure). We discuss the behavior of the ratios  $-\ln(R_n^{(f)})$  in Fig. 4 (bottom). Again, we consider only the case of adjacent intervals. The data for  $-\ln(R_n^{(f)})$  exhibit a linear behavior up to  $t/\ell \sim 0.5$ , reflecting that  $v_{\max} \sim 1$ . Similar to the bosonic case, finite-size corrections are present, although the analytical prediction in Eq. (25) is recovered in the scaling limit. In the inset, we also investigate these scaling corrections. The symbols are the data at fixed  $t/\ell = 0.5$  while the  $x$ -axis shows  $1/\ell$ . The crosses are the theoretical results in the scaling limit. The solid lines are fits to the behavior  $1/\ell$ , and are clearly consistent with the data.

We now remind that for free fermion systems (see section 2) it is not straightforward to compute the standard negativity defined from the partial transpose  $\rho_A^{T_1}$ . On the other hand, the Rényi negativities can be computed effectively. The reason is that the powers of  $\rho_A^{T_1}$  can be written as sum of products of gaussian operators (cf. Eq. (12)). Since each term of the sum is a gaussian operator, its trace can be effectively computed [82, 137]. For instance, for the Rényi negativity  $\mathcal{E}_3^{(b)}$ , we have to compute

$$\text{Tr}(\rho_A^{T_1})^3 = -\frac{1}{2}\text{Tr}(O_+^3) + \frac{3}{2}\text{Tr}(O_+^2 O_-). \quad (44)$$

By using Eq. (44) the ratio  $-\ln(R_3^{(b)})$  can be calculated and, for the quench with  $h_0 = 0.1 \rightarrow h = 2$ , is reported in Fig. 6. The symbols in the figure are numerical results for  $-\ln(R_3^{(b)})$  for two adjacent intervals of length  $\ell$ . The line is the quasiparticle prediction in Eq. (25). The good agreement between the data and the analytic curve confirms that  $-\ln(R_n^{(b)})$  and  $-\ln(R_n^{(f)})$

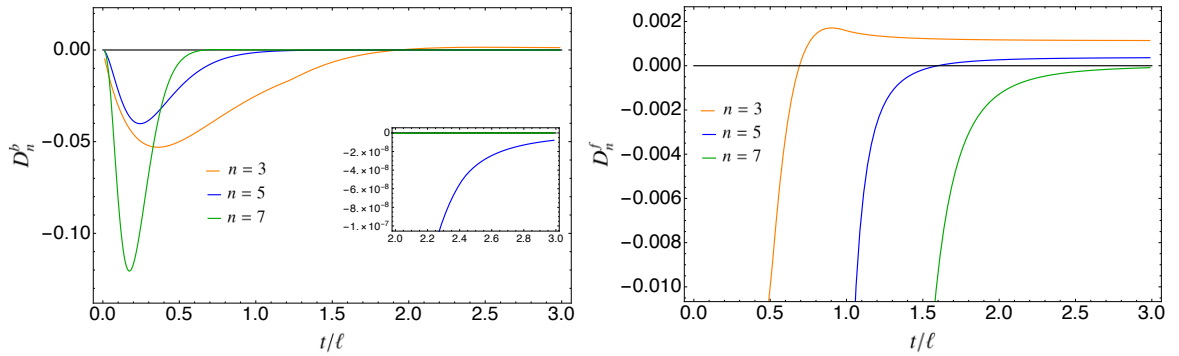


**Figure 7:** The  $p_n$ -PPT conditions for  $n = 3, 5, 7$  for the quasiparticle predictions of the moments of the partial transpose introduced in Eq. (15). The quench parameters are  $h_0 = 10, h = 2$  for the fermionic chain and  $m = 2, m_0 = 0.1$  for the harmonic chain. We plot the quantity  $D_n$  in Eq. (17). The  $p_n$ -PPT condition is  $D_n \geq 0$ . To compare data for different  $n$  we multiply the  $D_5$  by 10 and  $D_7$  by  $10^6$  for bosons ( $\ell = 30$ ). For fermions the  $D_5$  is multiplied by  $10^7$  and  $D_7$  by  $10^{19}$  ( $\ell = 50$ ). The violation of these conditions for at least one value of  $n$  reveals the presence of entanglement between  $A_1$  and  $A_2$ .

are the same in the space-time scaling limit. Interestingly, we observe that the fermionic Rényi negativity  $\mathcal{E}_3^{(f)}$  corresponds to the term  $\text{Tr}(O_+^2 O_-)$  in Eq. (44), as can be read in Eq. (14). The fact that the quasiparticle description correctly describes both  $\text{Tr}(O_+^2 O_-)$  and the weighted sum in Eq. (44), suggests that the terms in Eq. (44) become the same in the space-time scaling limit.

Finally, let us shortly discuss the connection between the reduced density matrices of fermionic and spin models that are connected by the Jordan-Wigner transformation. Due to the non-locality of this transformation, the reduced density matrices corresponding to  $A_1 \cup A_2$  in a spin chain model and its fermionic counterpart are usually not equivalent unless  $A_1$  and  $A_2$  are adjacent intervals [82, 89]. The same holds also for the (standard) transposed density matrices, for which the identity in Eq. (12) should be slightly modified to take into account the Jordan-Wigner string along the interval of length  $d$  connecting the two blocks in spin models.

### 5.3 Quasiparticle prediction for the $p_n$ -PPT conditions

Using the quasiparticle predictions obtained in the previous sections for the Rényi negativity, one can write down the quasiparticle formulas for the  $p_n$ -PPT conditions introduced in section 2.1, see Eq. (17). For instance, the  $p_3$ -PPT condition quantifies the violation of Eq. (16). Specifically, the condition  $D_3 \equiv p_3 - p_2^2 < 0$  signals the presence of quantum entanglement. As explained in section 2.1, other conditions  $D_n \geq 0$  can be obtained by considering higher moments of the partial transpose.

We numerically investigate the  $p_n$ -PPT conditions in Fig. 7 for  $n = 3, 5, 7$ , and for quenches in both the fermionic and harmonic chains. We focus on the situation with two adjacent intervals and we are interested in understanding how the  $p_n$ -PPT conditions are violated as a function of time. The results in Fig. 7 are obtained by using the quasiparticle picture prediction. As it is clear from the figure, all  $p_n$ -PPT conditions are violated at short times in both models. At infinite times all the  $p_n$ -PPT conditions give zero. These results are consistent with the behavior of the logarithmic negativity [19].

Also the fine structure of these  $p_n$ -PPT conditions is very interesting. In the short-time region with a lot of entanglement (compare with the previous figures for  $R_n$ ) all the conditions are violated. As the time increase and the entanglement becomes much less, the first condition to be satisfied is  $p_3$  (i.e.  $D_3 > 0$ ) and only after the other one (the panel on the left is particularly clear in this respect) This implies that higher and higher  $p_n$ -PPT conditions are necessary to



detect the very little amount of entanglement present at large time. This fact is not surprising, but it is remarkable that it is captured so neatly by the quasiparticle picture.

## 6 Conclusions

In this paper, we derived the quasiparticle picture for the dynamics of the moments of the partially transposed reduced density matrix after a quantum quench in integrable systems, and several related quantities such as the Rényi negativities  $\mathcal{E}_n$  (cf. Eq. (9)) and the ratios  $R_n$  (cf. Eq. (11)). An interesting result is that the ratio  $R_n$  is proportional to the Rényi mutual information. Furthermore, this ratio is qualitatively similar to the negativity and so it is then an indicator of the entanglement barrier for the quench dynamics at intermediate time [19, 140–142]. Moreover, our results allow us to derive the behavior of the  $p_n$ -PPT conditions, which in contrast with standard entanglement measures for mixed states, such as the logarithmic negativity, are easily computable and experimentally measurable for quantum many-body systems [15, 16]. We tested our predictions against exact numerical results for both free-fermion and free-boson systems.

We now discuss future research directions. The first natural followup of the results presented here is to test numerically the equality between Rényi mutual informations and the ratios  $R_n$  for interacting integrable models. A possible extension to this work would be to study the dynamics of negativity and the moments of the partial transpose in the presence of a globally conserved charge. While it is known that the negativity of two subsystems may be decomposed into contributions associated with their charge imbalance [18, 75], it would be interesting to understand whether a quasiparticle prediction similar to the one presented for the entropy in Ref. [131] could be worked out. Another important research direction is to investigate the Rényi negativities and the ratios  $R_n$  in the presence of dissipation [129].

## Acknowledgments

P.C. and S.M. acknowledge support from ERC under Consolidator grant number 771536 (NEMO). V.A. acknowledges support from the European Research Council under ERC Advanced grant No. 743032 DYNAMINT.

## References

- [1] P. Calabrese and J. Cardy, *Time Dependence of Correlation Functions Following a Quantum Quench*, *Phys. Rev. Lett.* **96**, 136801 (2006).
- [2] P. Calabrese and J. Cardy, *Quantum quenches in extended systems*, *J. Stat. Mech.* P06008 (2007).
- [3] P. Calabrese and J. Cardy, *Evolution of Entanglement Entropy in One-Dimensional Systems*, *J. Stat. Mech.* P04010 (2005).
- [4] V. Alba and P. Calabrese, *Entanglement and thermodynamics after a quantum quench in integrable systems*, *PNAS* **114**, 7947 (2017).
- [5] V. Alba and P. Calabrese, *Entanglement dynamics after quantum quenches in generic integrable systems*, *SciPost Phys.* **4**, 017 (2018).
- [6] P. Calabrese, *Entanglement spreading in non-equilibrium integrable systems*, *Lectures for Les Houches Summer School on "Integrability in Atomic and Condensed Matter Physics"*, *SciPost Phys. Lect. Notes* **20** (2020).

- [7] A. M. Kaufman, M. E. Tai, A. Lukin, M. Rispoli, R. Schittko, P. M. Preiss, and M. Greiner, *Quantum thermalisation through entanglement in an isolated many-body system*, [Science](#) **353**, 794 (2016).
- [8] A. Elben, B. Vermersch, M. Dalmonte, J.I. Cirac and P. Zoller, *Rényi Entropies from Random Quenches in Atomic Hubbard and Spin Models*, [Phys. Rev. Lett.](#) **120**, 050406 (2018).
- [9] T. Brydges, A. Elben, P. Jurcevic, B. Vermersch, C. Maier, B. P. Lanyon, P. Zoller, R. Blatt, and C. F. Roos, *Probing entanglement entropy via randomized measurements*, [Science](#) **364**, 260 (2019).
- [10] A. Lukin, M. Rispoli, R. Schittko, M. E. Tai, A. M. Kaufman, S. Choi, V. Khemani, J. Leonard, and M. Z. Greiner, *Probing entanglement in a many-body localized system*, [Science](#) **364**, 256 (2019).
- [11] A. Peres, *Separability Criterion for Density Matrices* [Phys. Rev. Lett.](#) **77**, 1413 (1996).
- [12] R. Simon, *Peres-Horodecki Separability Criterion for Continuous Variable Systems*, [Phys. Rev. Lett.](#) **84**, 2726 (2000).
- [13] G. Vidal and R. F. Werner, *A computable measure of entanglement*, [Phys. Rev. A](#) **65**, 032314 (2002).
- [14] M. B. Plenio, *Logarithmic Negativity: A Full Entanglement Monotone That is not Convex*, [Phys. Rev. Lett.](#) **95**, 090503 (2005);  
J. Eisert, *Entanglement in quantum information theory*, [Arxiv:quant-ph/0610253](#).
- [15] A. Elben, R. Kueng, H.-Y. Huang, R. van Bijnen, C. Kokail, M. Dalmonte, P. Calabrese, B. Kraus, J. Preskill, P. Zoller, and B. Vermersch, *Mixed-state entanglement from local randomized measurements*, [Phys. Rev. Lett.](#) **125**, 200501 (2020).
- [16] A. Neven, J. Carrasco, V. Vitale, C. Kokail, A. Elben, M. Dalmonte, P. Calabrese, P. Zoller, B. Vermersch, R. Kueng, and B. Kraus, *Symmetry-resolved entanglement detection using partial transpose moments*, [npj Quantum Inf.](#) **7**, 152 (2021).
- [17] J. Gray, L. Banchi, A. Bayat, and S. Bose, *Machine Learning Assisted Many-Body Entanglement Measurement*, [Phys. Rev. Lett.](#) **121**, 150503 (2018).
- [18] E. Cornfeld, E. Sela, and M. Goldstein, *Measuring fermionic entanglement: Entropy, negativity, and spin structure*, [Phys. Rev. A](#) **99**, 062309 (2019).
- [19] V. Alba and P. Calabrese, *Quantum information dynamics in multipartite integrable systems*, [EPL](#) **126**, 60001 (2019).
- [20] A. Coser, E. Tonni, and P. Calabrese, *Entanglement negativity after a global quantum quench*, [J. Stat. Mech.](#) P12017 (2014).
- [21] X. Wen, P.-Y. Chang, and S. Ryu, *Entanglement negativity after a local quantum quench in conformal field theories*, [Phys. Rev. B](#) **92**, 075109 (2015).
- [22] J. Kudler-Flam, H. Shapourian, and S. Ryu, *The negativity contour: a quasi-local measure of entanglement for mixed states*, [SciPost Phys.](#) **8**, 063 (2020).
- [23] P. Calabrese, J. Cardy, and E. Tonni, *Entanglement Negativity in Quantum Field Theory*, [Phys. Rev. Lett.](#) **109**, 130502 (2012).

- [24] P. Calabrese, J. Cardy, and E. Tonni, *Entanglement negativity in extended systems: a field theoretical approach*, *J. Stat. Mech.* P02008 (2013).
- [25] V. Alba, *Entanglement negativity and conformal field theory: a Monte Carlo study*, *J. Stat. Mech.* P05013 (2013).
- [26] C.-M. Chung, V. Alba, L. Bonnes, P. Chen, and A. M. Lauchli, *Entanglement negativity via replica trick: a Quantum Monte Carlo approach*, *Phys. Rev. B* **90**, 064401 (2014).
- [27] P. Calabrese, L. Tagliacozzo, and E. Tonni, *Entanglement negativity in the critical Ising chain*, *J. Stat. Mech.* P05002 (2013).
- [28] K.-H. Wu, T.-C. Lu, C.-M. Chung, Y.-J. Kao, and T. Grover, *Entanglement Renyi negativity across a finite temperature transition: a Monte Carlo study*, *Phys. Rev. Lett.* **125**, 140603 (2020).
- [29] T.-C. Lu and T. Grover, *Entanglement transitions as a probe of quasiparticles and quantum thermalization*, *Phys. Rev. B* **102**, 235110 (2020).
- [30] E. Wybo, M. Knap, and F. Pollmann, *Entanglement dynamics of a many-body localized system coupled to a bath*, *Phys. Rev. B* **102**, 064304 (2020).
- [31] L. Amico, R. Fazio, A. Osterloh, and V. Vedral, *Entanglement in many-body systems*, *Rev. Mod. Phys.* **80**, 517 (2008).
- [32] P. Calabrese, J. Cardy, and B. Doyon, *Entanglement entropy in extended quantum systems*, *J. Phys. A* **42**, 500301 (2009).
- [33] J. Eisert, M. Cramer, and M. B. Plenio, *Area laws for the entanglement entropy*, *Rev. Mod. Phys.* **82**, 277 (2010).
- [34] N. Laflorencie, *Quantum entanglement in condensed matter systems*, *Phys. Rep.* **643**, 1 (2016).
- [35] R. Islam, R. Ma, P. M. Preiss, M. E. Tai, A. Lukin, M. Rispoli and M. Greiner, *Measuring entanglement entropy in a quantum many-body system*, *Nature* **528**, 77 (2015).
- [36] V. Vitale, A. Elben, R. Kueng, A. Neven, J. Carrasco, B. Kraus, P. Zoller, P. Calabrese, B. Vermersch, and M. Dalmonte, *Symmetry-resolved dynamical purification in synthetic quantum matter*, [arXiv:2101.07814](https://arxiv.org/abs/2101.07814).
- [37] P. Calabrese and A. Lefevre, *Entanglement spectrum in one-dimensional systems*, *Phys. Rev. A* **78**, 032329(R) (2008).
- [38] C. G. Callan and F. Wilczek, *On Geometric Entropy*, *Phys. Lett. B* **333**, 55 (1994).
- [39] P. Calabrese and J. Cardy, *Entanglement entropy and quantum field theory*, *J. Stat. Mech.* P06002 (2004).
- [40] P. Calabrese and J. Cardy, *Entanglement entropy and conformal field theory*, *J. Phys. A* **42**, 504005 (2009).
- [41] M. Kormos and Z. Zimboras, *Temperature driven quenches in the Ising model: appearance of negative Rényi mutual information*, *J. Phys. A* **50**, 264005 (2017).
- [42] S. O. Scalet, A. M. Alhambra, G. Styliaris, and J. I. Cirac, *Computable Rényi mutual information: Area laws and correlations*, *Quantum* **5**, 541 (2021).

- [43] K. Audenaert, J. Eisert, M. B. Plenio, and R. F. Werner, *Entanglement properties of the harmonic chain*, *Phys. Rev. A* **66**, 042327 (2002)
- [44] A. Ferraro, D. Cavalcanti, A. García Saez, and A. Acín, *Thermal Bound Entanglement in Macroscopic Systems and Area Law*, *Phys. Rev. Lett.* **100**, 080502 (2008).
- [45] D. Cavalcanti, A. Ferraro, A. García Saez, and A. Acín, *Distillable entanglement and area laws in spin and harmonic-oscillator systems*, *Phys. Rev. A* **78**, 012335 (2008).
- [46] J. Anders and W. Andreas, *Entanglement and separability of quantum harmonic oscillator systems at finite temperature*, *Quantum Inf. Comput.* **8**, 0245 (2008).
- [47] J. Anders, *Thermal state entanglement in harmonic lattices*, *Phys. Rev. A* **77**, 062102 (2008).
- [48] S. Marcovitch, A. Retzker, M. B. Plenio, and B. Reznik, *Critical and noncritical long-range entanglement in Klein-Gordon fields*, *Phys. Rev. A* **80**, 012325 (2009).
- [49] V. Eisler and Z. Zimborás, *Entanglement negativity in the harmonic chain out of equilibrium*, *New J. Phys.* **16**, 123020 (2014).
- [50] N. E. Sherman, T. Devakul, M. B. Hastings, and R. R. P. Singh, *Nonzero-temperature entanglement negativity of quantum spin models: Area law, linked cluster expansions, and sudden death*, *Phys. Rev. E* **93**, 022128 (2016).
- [51] C. D. Nobili, A. Coser, and E. Tonni, *Entanglement negativity in a two dimensional harmonic lattice: area law and corner contributions*, *J. Stat. Mech.* 083102 (2016).
- [52] H. Wichterich, J. Molina-Vilaplana, and S. Bose, *Scaling of entanglement between separated blocks in spin chains at criticality*, *Phys. Rev. A* **80**, 010304 (2009).
- [53] A. Bayat, S. Bose, and P. Sodano, *Entanglement Routers Using Macroscopic Singlets*, *Phys. Rev. Lett.* **105**, 187204 (2010).
- [54] A. Bayat, S. Bose, P. Sodano, and H. Johannesson, *Entanglement Probe of Two- Impurity Kondo Physics in a Spin Chain*, *Phys. Rev. Lett.* **109**, 066403 (2012).
- [55] H. Wichterich, J. Vidal, and S. Bose, *Universality of the negativity in the Lipkin-Meshkov-Glick model*, *Phys. Rev. A* **81**, 032311 (2010).
- [56] R. A. Santos, V. Korepin, and S. Bose, *Negativity for two blocks in the one-dimensional spin-1 Affleck-Kennedy-Lieb-Tasaki model*, *Phys. Rev. A* **84**, 062307 (2011).
- [57] A. Bayat, P. Sodano, and S. Bose, *Negativity as the entanglement measure to probe the Kondo regime in the spin-chain Kondo model*, *Phys. Rev. B* **81**, 064429 (2010).
- [58] T. C. Lu, and T. Grover, *Singularity in Entanglement Negativity Across Finite Temperature Phase Transitions*, *Phys. Rev. B* **99**, 075157 (2019).
- [59] P. Ruggiero, V. Alba, and P. Calabrese, *Entanglement negativity in random spin chains*, *Phys. Rev. B* **94**, 035152 (2016).
- [60] X. Turkeshi, P. Ruggiero, and P. Calabrese, *Negativity Spectrum in the Random Singlet Phase*, *Phys. Rev. B* **101**, 064207 (2020).
- [61] G. B. Mbeng, V. Alba, and P. Calabrese, *Negativity spectrum in 1D gapped phases of matter*, *J. Phys. A* **50**, 194001 (2017).

- [62] S. Wald, R. Arias, and V. Alba, *Entanglement and classical fluctuations at finite-temperature critical points*, *J. Stat. Mech.* (2020) 033105.
- [63] H. Shapourian, S. Liu, J. Kudler-Flam, and A. Vishwanath, *Entanglement negativity spectrum of random mixed states: A diagrammatic approach*, *PRX Quantum* **2**, 030347 (2021).
- [64] P. Calabrese, J. Cardy, and E. Tonni, *Finite temperature entanglement negativity in conformal field theory*, *J. Phys. A* **48**, 015006 (2015).
- [65] P. Ruggiero, V. Alba, and P. Calabrese, *Negativity spectrum of one-dimensional conformal field theories*, *Phys. Rev. B* **94**, 195121 (2016).
- [66] V. Alba, P. Calabrese, and E. Tonni, *Entanglement spectrum degeneracy and the Cardy formula in 1+1 dimensional conformal field theories*, *J. Phys. A* **51**, 024001 (2018).
- [67] M. Kulaxizi, A. Parnachev, and G. Policastro, *Conformal blocks and negativity at large central charge*, *JHEP* **09**, 010 (2014).
- [68] C. De Nobili, A. Coser, and E. Tonni, *Entanglement entropy and negativity of disjoint intervals in CFT: Some numerical extrapolations*, *J. Stat. Mech.* (2015) P06021.
- [69] D. Bianchini and O. A. Castro-Alvaredo, *Branch point twist field correlators in the massive free Boson theory*, *Nucl. Phys. B* **913**, 879 (2016).
- [70] O. Blondeau-Fournier, O. A. Castro-Alvaredo, and B. Doyon, *Universal scaling of the logarithmic negativity in massive quantum field theory*, *J. Phys. A* **49**, 125401 (2016).
- [71] O. A. Castro-Alvaredo, C. De Fazio, B. Doyon, and I. M. Szecsenyi, *Entanglement Content of Quantum Particle Excitations II. Disconnected Regions and Logarithmic Negativity*, *JHEP* **11** (2019) 58.
- [72] O. A. Castro-Alvaredo, C. De Fazio, B. Doyon, and I. M. Szecsenyi, *Entanglement Content of Quantum Particle Excitations III. Graph Partition Functions*, *J. Math. Phys.* **60**, 082301 (2019).
- [73] J. Kudler-Flam and S. Ryu, *Entanglement negativity and minimal entanglement wedge cross sections in holographic theories*, *Phys. Rev. D* **99**, 106014 (2019).
- [74] F. Ares, R. Santachiara, and J. Viti, *Crossing-symmetric Twist Field Correlators and Entanglement Negativity in Minimal CFTs*, *JHEP* **10** (2021) 175
- [75] S. Murciano, R. Bonsignori, and P. Calabrese, *Symmetry decomposition of negativity of massless free fermions*, *SciPost Phys.* **10**, 111 (2021).
- [76] V. Eisler and Z. Zimborás, *Entanglement negativity in the harmonic chain out of equilibrium*, *New J. Phys.* **16**, 123020 (2014).
- [77] M. Hoogeveen and B. Doyon, *Entanglement negativity and entropy in non-equilibrium conformal field theory*, *Nucl. Phys. B* **898**, 78 (2015).
- [78] M. J. Gullans and D. A. Huse, *Entanglement Structure of Current-Driven Diffusive Fermion Systems*, *Phys. Rev. X* **9**, 021007 (2019).
- [79] J. Kudler-Flam, Y. Kusuki, and S. Ryu, *Correlation measures and the entanglement wedge cross-section after quantum quenches in two-dimensional conformal field theories*, *JHEP* **04**, 074 (2020).

- [80] J. Kudler-Flam, Y. Kusuki, and S. Ryu, *The quasi-particle picture and its breakdown after local quenches: mutual information, negativity, and reflected entropy*, *JHEP* **03** (2021) 146.
- [81] B. Shi, X. Dai, and Y.-M. Lu, *Entanglement negativity at the critical point of measurement-driven transition*, [ArXiv:2012.00040](#).
- [82] V. Eisler and Z. Zimborás, *On the partial transpose of fermionic Gaussian states*, *New J. Phys.* **17**, 053048 (2015).
- [83] A. Coser, E. Tonni and P. Calabrese *Towards the entanglement negativity of two disjoint intervals for a one dimensional free fermion*, *J. Stat. Mech.* 033116 (2016).
- [84] A. Coser, E. Tonni, and P. Calabrese, *Spin structures and entanglement of two disjoint intervals in conformal field theories*, *J. Stat. Mech.* 053109 (2016).
- [85] V. Eisler and Z. Zimborás, *Entanglement negativity in two-dimensional free lattice models*, *Phys. Rev. B* **93**, 115148 (2016).
- [86] P.-Y. Chang and X. Wen, *Entanglement negativity in free-fermion systems: An overlap matrix approach*, *Phys. Rev. B* **93**, 195140 (2016).
- [87] C. P. Herzog and Y. Wang, *Estimation for entanglement negativity of free fermions*, [YITP-SB-15-17](#) (2016).
- [88] J. Eisert, V. Eisler, and Z. Zimborás, *Entanglement negativity bounds for fermionic Gaussian states*, *Phys. Rev. B* **97**, 165123 (2018).
- [89] A. Coser, E. Tonni, and P. Calabrese *Partial transpose of two disjoint blocks in XY spin chains*, *J. Stat. Mech.* P08005 (2015).
- [90] H. Shapourian, K. Shiozaki, and S. Ryu, *Many-Body Topological Invariants for Fermionic Symmetry-Protected Topological Phases*, *Phys. Rev. Lett.* **118**, 216402 (2017).
- [91] K. Shiozaki, H. Shapourian, K. Gomi, and S. Ryu, *Many-body topological invariants for fermionic short-range entangled topological phases protected by antiunitary symmetries*, *Phys. Rev. B* **98**, 035151 (2018).
- [92] H. Shapourian and S. Ryu, *Entanglement negativity of fermions: monotonicity, separability criterion, and classification of few-mode states*, *Phys. Rev. A* **99**, 022310 (2019).
- [93] H. Shapourian, K. Shiozaki, and S. Ryu, *Partial time-reversal transformation and entanglement negativity in fermionic systems*, *Phys. Rev. B* **95**, 165101 (2017).
- [94] H. Shapourian and S. Ryu, *Finite-temperature entanglement negativity of free fermions*, *J. Stat. Mech.* 043106 (2019).
- [95] H. Shapourian, P. Ruggiero, S. Ryu, and P. Calabrese, *Twisted and untwisted negativity spectrum of free fermions*, *SciPost Phys.* **7**, 037 (2019).
- [96] H. Shapourian, R. S. K. Mong, and S. Ryu, *Anyonic Partial Transpose I: Quantum Information Aspects*, [arXiv:2012.02222](#).
- [97] J. L. Cardy, O. A. Castro-Alvaredo, and B. Doyon, *Form factors of branch-point twist fields in quantum integrable models and entanglement entropy*, *J. Stat. Phys.* **130**, 129 (2008).
- [98] B. Bertini, E. Tartaglia, and P. Calabrese, *Quantum Quench in the Infinitely Repulsive Hubbard Model: The Stationary State*, *J. Stat. Mech.* (2017) 103107.

- [99] B. Bertini, E. Tartaglia, and P. Calabrese, *Entanglement and diagonal entropies after a quench with no pair structure*, *J. Stat. Mech.* (2018) 063104.
- [100] A. Bastianello and P. Calabrese, *Spreading of entanglement and correlations after a quench with intertwined quasiparticles*, *SciPost Phys.* **5**, 033 (2018).
- [101] A. Bastianello and M. Collura, *Entanglement spreading and quasiparticle picture beyond the pair structure*, *SciPost Phys.* **8**, 045 (2020).
- [102] L. Piroli, B. Pozsgay, and E. Vernier, *What is an integrable quench?*, *Nucl. Phys. B* **925**, 362 (2017).
- [103] M. Fagotti and P. Calabrese, *Evolution of entanglement entropy following a quantum quench: Analytic results for the XY chain in a transverse magnetic field*, *Phys. Rev. A* **78**, 010306 (2008).
- [104] P. Calabrese, F. H. L. Essler, and G. Mussardo, *Introduction to “Quantum Integrability in Out of Equilibrium Systems”*, *J. Stat. Mech.* 064001 (2016).
- [105] L. Vidmar and M. Rigol, *Generalized Gibbs ensemble in integrable lattice models*, *J. Stat. Mech.* 064007 (2016).
- [106] F. H. L. Essler and M. Fagotti, *Generalized Gibbs ensemble in integrable lattice models*, *J. Stat. Mech.* 064002 (2016).
- [107] L. Bonnes, F.H.L. Essler, and A. M. Läuchli, *Light-cone dynamics after quantum quenches in spin chains*, *Phys. Rev. Lett.* **113**, 187203 (2014).
- [108] M. Mestyán, B. Bertini, L. Piroli, and P. Calabrese, *Exact solution for the quench dynamics of a nested integrable system*, *J. Stat. Mech.* (2017) 083103
- [109] L. Piroli, E. Vernier, P. Calabrese, and B. Pozsgay, *Integrable quenches in nested spin chains I: the exact steady states*, *J. Stat. Mech.* (2019) 063103.
- [110] L. Piroli, E. Vernier, P. Calabrese, and M. Rigol, *Correlations and diagonal entropy after quantum quenches in XXZ chains*, *Phys. Rev. B* **95**, 054308 (2017)
- [111] R. Modak, L. Piroli, and P. Calabrese, *Correlations and entanglement spreading in nested spin chains*, *J. Stat. Mech.* (2019) 093106.
- [112] V. Alba and P. Calabrese, *Quench action and Rényi entropies in integrable systems*, *Phys. Rev. B* **96**, 115421 (2017).
- [113] V. Alba and P. Calabrese, *Rényi entropies after releasing the Néel state in the XXZ spin-chain*, *J. Stat. Mech.* 113105 (2017).
- [114] M. Mestyán, V. Alba, and P. Calabrese, *Rényi entropies of generic thermodynamic macrostates in integrable systems*, *J. Stat. Mech.* 083104 (2018).
- [115] K. Klobas, B. Bertini, and L. Piroli, *Exact thermalization dynamics in the “Rule 54” Quantum Cellular Automaton*, *Phys. Rev. Lett.* **126**, 160602 (2021).
- [116] K. Klobas and B. Bertini, *Entanglement dynamics in Rule 54: Exact results and quasiparticle picture*, [arXiv:2104.04513](https://arxiv.org/abs/2104.04513).
- [117] V. Alba and P. Calabrese, *Quantum information scrambling after a quantum quench*, *Phys. Rev. B* **100**, 115150 (2019).

- [118] R. Modak, V. Alba, and P. Calabrese, *Entanglement revivals as a probe of scrambling in finite quantum systems*, *J. Stat. Mech.* **083110** (2020).
- [119] O. A. Castro-Alvaredo, B. Doyon, and T. Yoshimura, *Emergent Hydrodynamics in Integrable Quantum Systems Out of Equilibrium*, *Phys. Rev. X* **6**, 041065 (2016).
- [120] B. Bertini, M. Collura, J. De Nardis, and M. Fagotti, *Transport in Out-of-Equilibrium XXZ Chains: Exact Profiles of Charges and Currents*, *Phys. Rev. Lett.* **117**, 207201 (2016)
- [121] V. Alba, *Towards a Generalized Hydrodynamics description of Rényi entropies in integrable systems*, *Phys. Rev. B* **99**, 045150 (2019).
- [122] V. Alba, *Entanglement and quantum transport in integrable systems*, *Phys. Rev. B* **97**, 245135 (2018).
- [123] V. Alba, B. Bertini, and M. Fagotti, *Entanglement evolution and generalised hydrodynamics: interacting integrable systems*, *SciPost Phys.* **7**, 005 (2019).
- [124] B. Bertini, M. Fagotti, L. Piroli, and P. Calabrese, *Entanglement evolution and generalised hydrodynamics: noninteracting systems*, *J. Phys. A* **51**, 39LT01 (2018).
- [125] M. Mestyán and V. Alba, *Molecular dynamics simulation of entanglement spreading in generalized hydrodynamics*, *SciPost Phys.* **8**, 055 (2020).
- [126] V. Alba, B. Bertini, M. Fagotti, L. Piroli, and P. Ruggiero, *Generalized-Hydrodynamic approach to Inhomogeneous Quenches: Correlations, Entanglement and Quantum Effects*, [arXiv:2104.00656](https://arxiv.org/abs/2104.00656).
- [127] V. Alba, *Unbounded entanglement production via a dissipative impurity*, [arXiv:2104.10921](https://arxiv.org/abs/2104.10921).
- [128] V. Alba and F. Carollo, *Spreading of correlations in Markovian open quantum systems*, *Phys. Rev. B* **103**, 020302 (2021).
- [129] F. Carollo and V. Alba, *Emergent dissipative quasi-particle picture in noninteracting Markovian open quantum systems*, [arXiv:2106.11997](https://arxiv.org/abs/2106.11997).
- [130] V. Alba and F. Carollo, *Hydrodynamics of quantum entropies in Ising chains with linear dissipation*, [arXiv:2109.01836](https://arxiv.org/abs/2109.01836).
- [131] G. Perez, R. Bonsignori, and P. Calabrese *Quasiparticle dynamics of symmetry-resolved entanglement after a quench: Examples of conformal field theories and free fermions*, *Phys. Rev. B* **103**, L041104 (2020).
- [132] G. Perez, R. Bonsignori, P. Calabrese, *Exact quench dynamics of symmetry resolved entanglement in a free fermion chain*, *J. Stat. Mech.* (2021) 093102.
- [133] B. Bertini and P. Calabrese, *Prethermalisation and Thermalisation in the Entanglement Dynamics*, *Phys. Rev. B* **102**, 094303 (2020)
- [134] P. Calabrese, *Entanglement and thermodynamics in non-equilibrium isolated quantum systems*, *Physica A* **504**, 31 (2018).
- [135] V. Eisler and I. Peschel, *Reduced density matrices and entanglement entropy in free lattice models*, *J. Phys. A* (2009) **42** 504003 (2009).
- [136] F. Igloi and I. Peschel, *On reduced density matrices for disjoint subsystems*, *EPL* **89**, 40001 (2010).



- [137] M. Fagotti and P. Calabrese, *Entanglement entropy of two disjoint blocks in XY chains*, *J. Stat. Mech.* P04016 (2010).
- [138] P. Calabrese, F. H. L. Essler, and M. Fagotti, *Quantum Quench in the Transverse-Field Ising Chain*, *Phys. Rev. Lett.* **106**, 227203 (2011).
- [139] P. Calabrese, F. H. L. Essler, and M. Fagotti, *Quantum Quench in the Transverse Field Ising chain I: Time evolution of order parameter correlators*, *J. Stat. Mech.* P07016 (2012).
- [140] J. Dubail, *Entanglement scaling of operators: a conformal field theory approach, with a glimpse of simulability of long-time dynamics in 1+1d*, *J. Phys. A* **50**, 234001 (2017).
- [141] E. Leviatan, F. Pollmann, J. H. Bardarson, D. A. Huse, and E. Altman, *Quantum thermalization dynamics with Matrix-Product States*, [arXiv:1702.08894](https://arxiv.org/abs/1702.08894).
- [142] C. Jonay, D. A. Huse, and A. Nahum, *Coarse-grained dynamics of operator and state entanglement*, [arXiv:1803.00089](https://arxiv.org/abs/1803.00089).